Available online on 30.08.2019 at http://jddtonline.info

Journal of Drug Delivery and Therapeutics

Open Access to Pharmaceutical and Medical Research

Open Access Research Article

Synthesis, Characterization and Evaluation of Anticancer Activity of Nanoresveratrol in B16 Melanoma Cell Line

Arora Reena [1] & Parkash Chander [1*]

[1] Department of Chemical Sciences, IKG Punjab Technical University, Kapurthala, Punjab

ABSTRACT

Resveratrol, a member of the stilbene family, is a naturally occurring polyphenolic compound in grapes and other botanicals. It carries a potential to prevent or treat several chronic diseases, including cancers. Despite various promising health benefits, including chemopreventive and chemotherapeutic benefits against cancer, clinical translation of resveratrol is hampered due to its poor bioavailability, solubility and stability. Here we present the study to prepare nano-formulation of resveratrol for improving the resveratrol profile. Calcium phosphate loaded nanoresveratrol has been synthesized, characterized and its anti-proliferative effects were examined in a B16 murine melanoma cell line. The anti-cancer effects of nanoresveratrol were directly compared with free resveratrol and chemotherapy drug 5-FU. Nanoresveratrol induced apoptosis in B16 melanoma more efficiently as compared to resveratrol alone and 5 FU. A nuclear staining profile following Hoechst staining of B16 cells is indicative of apoptosis and shows that the anti-cancer effect of nanoresveratrol is due to apoptosis induction. Since antioxidant activity is a hallmark of resveratrol, we also measured the biochemical antioxidant activities of superoxide dismutase (SOD) and catalase antioxidant enzymes. We found that, concurrent with the anti-cancer activity, the antioxidant activity of nanoresveratrol increased. Collectively, these findings clearly show that nanoresveratrol is superior to free resveratrol in suppressing cell growth in B16 murine melanoma cell line, and that the anti-cancer activity is primarily through apoptosis induction.

Keywords: Resveratrol, Nanoresveratrol, Formulation, B16 cell line, Cancer, Melanoma, Chemopreventive, Chemotherapeutic

Article Info: Received 19 June 2019; Review Completed 17 Aug 2019; Accepted 20 Aug 2019; Available online 30 Aug 2019

Cite this article as:

Arora R, Parkash C, Synthesis, Characterization and Evaluation of Anticancer Activity of Nanoresveratrol in B16 Melanoma Cell Line , Journal of Drug Delivery and Therapeutics. 2019; 9(4-A):625-631
http://dx.doi.org/10.22270/jddt.v9i4-A.3521

***Address for Correspondence:**

Dr Chander Parkash, Institution Name: Department of Chemical Sciences, I.K.G. Punjab Technical University, Kapurthala, Punjab 144603, India

1. INTRODUCTION

Resveratrol (chemically: 3,5,4'-trihydroxystilbene) a member of stilbene family, is a naturally occurring polyphenolic compound present in grapes, berries, peanuts and red wine. It is a very well-known antioxidant and exhibits various biological effects including anticancer, antiangiogenic, immunomodulatory and cardioprotective activities [1,2,3]. Its beneficial potential in a variety of indications includes the chemoprotective & chemotherapeutic effects in several cancers [4]. Resveratrol has been reported to have a role in reducing the growth of human cancers originating from diverse organs/sites, including breast, cervix, ovary, uterine, kidney, liver, eye, bladder, thyroid, oesophagus, prostate, brain, lung, skin, gastric, colon, head and neck, bone and blood [5-13]. Several studies indicate that resveratrol shows multiple anticancer effects such as protection against tumour initiation and cancer progression, apoptosis, antioxidant, anti-angiogenesis, anti-inflammatory, and antitumor migration [6-13]. Evidence show that resveratrol exerts its effects through different signalling pathways and several molecular players. Various studies report that resveratrol has a range of cellular effects, including cell cycle, invasion/metastasis, angiogenesis, apoptosis and autophagy. Several molecular players, such as BCL-2/BAX and AMPK, PI3K/AKT/mTOR, WNT, MEK, ERK pathways mediate resveratrol-induced cellular effects in different cancers [14]. However, the precise mechanisms remain to be delineated. There are several reports indicating the promising effects of resveratrol in treatment of skin cancer [15,16,17]. A recent report shows that resveratrol induces mitochondrial apoptosis in melanoma cell line through downregulating Bcl-2, activating BAX leading to apoptosis [18]. Additionally, this report also showed that pyruvate kinase PKM2 played a role in apoptosis through interacting with Bcl-2.

Despite widely established promising health benefits of resveratrol and its potential as a chemo preventive and chemotherapeutic agent in cancer based on in vitro and preclinical studies against several human cancers, its clinical translation remains challenging. Key challenges associated with the therapeutic application of resveratrol include poor solubility, stability and limited bioavailability [19,20].

Nanotechnology offers a wide range of innovative strategies to address the challenges associated with resveratrol. Plant metabolites can be incorporated into nano structures so that

they interact with biomolecules both inside the cell and on the surface of cells. With the coming of vast array of numerous novel nanosized delivery systems, it has paved a path for the development of various nano assemblies. These strategies have led to recent advances in formulation of nanoparticulate systems for various natural polyphenols targeted therapy and enhanced bioavailability with lowered adverse effects**.** Accumulating evidence reports a diverse kind of synthetic carriers or non-viral vectors for drug delivery. These carriers include liposome [21] lipid nanoparticles, [22] polymeric nanoparticles such as proteins [23] polymeric micelles [24] and hydrogels [25]. Calcium phosphate nanoparticles of size up to 100 nm in diameter have been used as carriers for the delivery of genes and drugs in animal cells with a relatively higher transfection efficiency compared to liposomal carriers [27, 28]. Improved formulations and drug delivery strategies can address the challenges associated with resveratrol [29-33]. In this study, we have synthesized and characterized calcium phosphate-encapsulated nanoresveratrol and performed a comparative evaluation of the anti-cancer activity of nanoresveratrol, free resveratrol and clinically used chemotherapy drug 5-Fluorouracil (5-FU). The ability of the free and encapsulated resveratrol to induce apoptosis in B16 melanoma cell line was evaluated. Since resveratrol is a well-known antioxidant, this activity was also examined.

2. MATERIALS AND METHODS

2.1 Chemicals

Di-sodium hydrogen phosphate, Tris–HCl buffer, Buffer tablets (pH 4.0 and pH 8.0) and n-Hexane (AR grade) were obtained from Rankem (India). Calcium chloride, Gel loading dye and Ethidium bromide were obtained from ACROS Chem. (USA). The surfactant i.e. Sodium bis-(2-ethylhexyl) sulfosuccinate (AR grade) was obtained as 99% pure product from Sigma (USA).

2.2 Cells and Reagents

B16 murine melanoma cell line was a kind gift from the Department of Biotechnology, Jamia Hamdard. B16 cell line was cultured in RPMI-1640 with 10% Fetal bovine serum (Gibco-BRL, Grand Island, NY, USA) at 37°C under 5% CO_2 humidified atmosphere. Resveratrol, Propidium Iodide, Hoechst 33342 and 5-Flurouracil were purchased from Sigma.

2.3 Synthesis of Calcium Phosphate loaded Nanoresveratrol

Nanoresveratrol loaded Calcium phosphate (CaP) nanoparticles were prepared in the aqueous core of an AOT (Aerosol-OT)/hexane/water reverse micellar system followed by the procedure described in the literature with some modifications [34]. In a typical set, 25 ml of 0.1 M AOT solution in hexane was prepared into which 70 µl aqueous solution of 1.36 M Calcium chloride and 50 µl stock solution of resveratrol was added with continuous stirring for 12 hours to form reverse micelle A. In another set of 25 ml of 0.1 M AOT/hexane solution, 50 µl of 0.2 M Tris–HCl buffer (pH 7.4) and 70 µl aqueous solution of 0.35 M Na_2HPO_4 was added with continuous stirring for 12 hours to form reverse micelle B. A calculated amount of excess water was added to each of the reverse micelles to make a total volume of added water to 250 ml in order to adjust Wo, i.e. the molar ratio of water to surfactant, to 10. Stirring was continued until both the reverse micelles A and B will become optically clear. Reverse micelle B, were then, added to reverse micelle A at an extremely slow rate with continuous stirring. The resulting mixture was further stirred for another 12 hours under the above cold conditions. The nanoparticles were found to remain dispersed at least for 24 h at room temperature after which the particles start settling at the bottom. Five ml of absolute ethanol (99.9% v/v) was added to break the reverse micelles into oil and aqueous phases. The particles were then separated by centrifugation of the aqueous phase at 12000 rpm. The particles were collected and dispersed in 95% v/v ethanol by sonication in a water bath sonicator. The ethanol solution was again centrifuged, and the particles were collected. Finally, the pelleted nanoparticles were dispersed in 5ml double distilled water by sonication for 15 min to prepare a clear dispersion. The dispersed nanoparticles were dialyzed overnight using a 12 kD cut off dialysis membrane bag. After dialysis, the resultant solution was lyophilized to get the dry sample.

2.4 Electron Microscopy

Size and shape of the nanoparticles was characterized through negative staining of the nanoparticles [35,36] followed by observation under a transmission electron microscope (Morgnani). Measurements were made using a computerized image analyzer and average size of the nanoparticles was noted.

2.5 Dynamic Light Scattering

DLS was used to determine the particle size distribution of the synthesized nanoparticles. The Malvern Zetasizer 3000HS was used to determine the size, size distribution and zeta potential of CaP nanoparticles at 25°C.1mg of the nanoparticles was dispersed in 2ml distilled water. Size and zeta potential were measured at 1.34 refractive index and 0.2 absorbance. The size distribution obtained from photon correlation spectroscopy (PCS) is based on the intensity of scattered light.

2.6 X-ray Diffraction Studies

Crystalline characteristics of the particles was studied by X-ray diffraction (XRD) studies. XRD were carried out on a Bruker D8 advance X-ray diffractometer using Ni-filtered Cu-Kα radiation. Normal scans were typically having a step of 0.02° with step time of 1sec over the range of 2θ=5-60°. Two mg of lyophilized nanoparticles were used for XRD analysis.

2.7 Cell Toxicity Studies

Equal number of cells were seeded and grown on cover slips in 6-well and 12 well plates (TPP, Switzerland) containing serum-free medium until they were sub-confluent. Resveratrol loaded calcium phosphate nanoparticles were used for the cell toxicity study. The concentrated nanoparticles were diluted in sterile autoclaved water. Nanoparticles at desired concentration were added to the cell culture. The cells were then incubated with the nanoparticles for 6h and 12h respectively. In the control group, cells were not treated with nanoparticles but were incubated for the same time periods. The cells were also treated with the same concentration of 5-Fluorouracil. Before terminating the culture, 500µl of the culture supernatant was collected from each well for further biochemical assays. The cells were then incubated for 15 minutes with the fluorescent stains Hoechst 33342 at a working dilution of 5mM and propidium iodide at a final concentration of 50µg/ml to discriminate dead and live cells. Hoechst is a nuclear stain that labels the nuclei blue and it is routinely used to assess apoptosis [37,38]. A characteristic feature of a cell undergoing apoptosis is chromatin condensation and the apoptotic cells appear strong bright blue, while normal healthy cells appear uniform blue. Hoechst 33342 can enter intact cells without need for cell

membrane permeabilization which helps in the identification of early apoptotic cells.

PI was then added to discriminate the early apoptotic population from the background of dead or very late apoptotic cells. PI can enter only those cells in which the cell membrane has been damaged as in dead cells or very late apoptotic cells. The cells were then washed in PBS three times for 5 minutes each and the cover slips were mounted on slides with 10% glycerol in PBS. The cells were immediately observed under an upright fluorescent microscope (Nikon Eclipse 600) using 488nm and 350nm filters. Images were captured using an Olympus DP-71 digital camera mounted on the microscope. Ten different fields were captured at 40X and cell counts were taken within each microscopic field to get statistically significant counts for apoptotic cells and viable cells. PI-stained cells were also counted to count dead cells. The apoptotic cells were quantitated as a percentage of the total cell count.

2.8 DNA Fragmentation Assay

Briefly, after completion of the experimental protocol, the cells were scraped using a cell scraper (TPP) and collected in 1.5 ml Eppendorf tubes. Lysis buffer (55µl volume) was added to each tube, followed by incubation of each sample for 20 minutes on ice. The tubes were centrifuged at 12,000g for 30 minutes at 4°C. The supernatant was collected, and DNA was isolated by routine phenol-chloroform extraction and cold ethanol precipitation. The DNA was quantitated, and equal quantities of DNA were dissolved in 30µl deionised water containing RNAse and 5µl loading buffer and kept for 30 minutes at 37°C. The samples were loaded on a 2% agarose gel containing ethidium bromide with molecular weight marker on the outer lane. After running the samples, the gel was observed under UV light in a transilluminator.

2.9 Biochemical Assays

Biochemical assays were carried out for studying the oxidative stress levels of B16 cells after incubation with the nanoparticles. Endogenous antioxidant levels of Superoxide dismutase (SOD) and catalase (CAT) were determined in the cell culture supernatants as reported previously [39] and briefly described below.

2.9.1 SOD Assay: A total volume of 100 µl culture supernatant was added to Sodium pyrophosphate buffer (pH-8.3) followed by addition of 0.1 ml of 186 µM Phenazine methosulphate, 0.3 ml of 300 mM Nitroblue tetrazolium and 0.2 ml of 780 µM NADH. Reaction mixture was incubated for 90 sec. at 30°C and stopped the reaction by adding 1.0 ml of glacial acetic acid. 4.0 ml of n-butanol was then added and centrifuged at 3,000 × g for 10 min. The absorbance of organic layer was measured at 560 nm.

2.9.2 Catalase Assay: Briefly, 50 µl culture supernatant was added to a 3.0 ml cuvette that contained 1.95 ml of 50 mM phosphate buffer (pH-7.0). Then 1.0 ml of 30 mM hydrogen peroxide was added and changes in absorbance were measured for 30 sec. at 240 nm at an interval of 15 sec.

3. RESULTS AND DISCUSSION

Synthesis of Calcium phosphate loaded nanoresveratrol was performed as described above. Structures of the synthesized formulation were characterized by TEM, DLS & X Ray crystallography. The characterized nanoresveratrol was evaluated for the cell toxicity against B16 melanoma cell line though PI staining, apoptosis induction through DNA condensation and fragmentation studies, and antioxidant activity using SOD and Catalase assays.

3.1 Physical Characterization of Nanoparticles-Transmission Electron Microscopic (TEM)

Size and morphology of the nanoparticles were determined by TEM as follows: one drop of the aqueous dispersion of CaP nanoparticles followed by one drop of 1% phosphotungstic acid were put on a formvar coated copper grid (1% solution of formvar was prepared in spectroscopic grade chloroform) and then air dried in a vacuum desiccator. The dried grid was examined under JEOL JEM 2000 EX 200 model electron microscope unit at All India Institute of Medical Sciences (AIIMS), New Delhi, India.

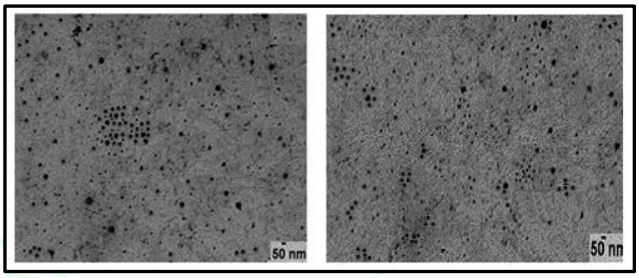

Fig 1(a) **Fig 1(b)**

Figure1. TEM images of Calcium Phosphate Nanoparticles a) loaded with resveratrol; b) void nanoparticles. *Resveratrol loaded calcium phosphate nanoparticles and void calcium phosphate nanoparticles revealed that the particles were mostly below 50 nm diameters and with spherical morphology.*

In our study we prepared CaP nanoparticles in the reverse micelles of Wo=10 and the size of nanoparticles ranging between 15-35 nm with average size around 20nm diameter, as shown in Fig 1. The TEM picture of Resveratrol loaded calcium phosphate nanoparticles and void calcium phosphate nanoparticles revealed that the particles were mostly below 50 nm diameters and with spherical morphology.

The nanoparticles were prepared according to the present protocol at Wo=10. The size of the nanoparticles can be controlled not only by Wo but also by temperature and stirring time. In our experiment the entire synthetic protocol was performed in the cold room at 4ºC and the stirring was done for 12hrs. Higher temperature and longer duration of stirring, however, increase the particle size accordingly.

3.2 Dynamic Light Scattering Studies

The TEM result was further confirmed by measuring the size of aqueous dispersed particles using Malvern Zetasizer 3000HS. DLS studies revealed the size range of 15-32nm with maximum population of 20-25nm size particles (Fig 2). The size distribution obtained from photon correlation spectroscopy (PCS) is based on the intensity of scattered light. The average size of the nanoparticles was found to be marginally different from that obtained by electron microscopy.

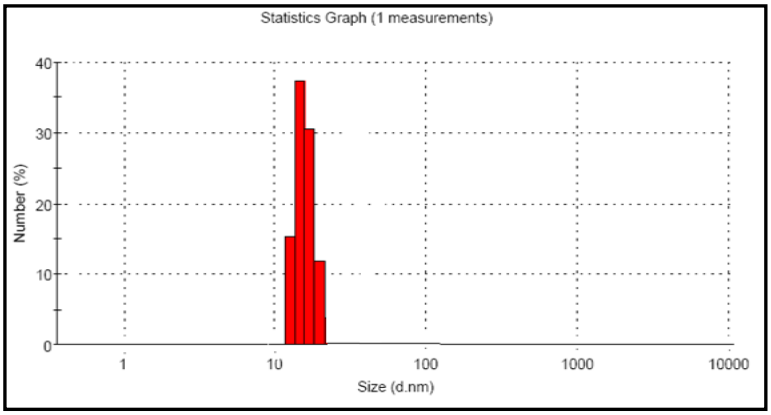

Figure 2. Dynamic Light Scattering experiment showing size and size distribution of loaded CaP nanoparticles. *The size range of 15-32nm with maximum population of 20-25nm size particles*

3.3 X-Ray Diffraction Studies

X-Ray diffraction studies were performed to study the crystalline characteristics of Calcium phosphate nanoparticles. Diffractograph of resveratrol loaded calcium phosphate nanoparticles synthesized at 4°C are crystalline in nature (Fig. 3).

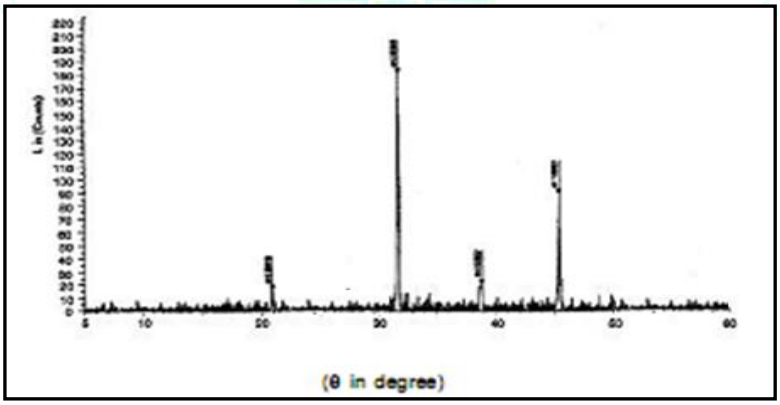

Figure 3. Powder XRD pattern of Resveratrol loaded Calcium Phosphate Nanoparticles. *A characteristic peak of 2θ=31.8 degree showed the formation of hydroxyapatite [$Ca_{10}(PO_4)_6(OH)_2$] crystals.*

3.4 Anticancer Activity

To determine the effect of the characterized nanoparticles on B16 cell survival, we performed different studies to examine the anti-cancer effect of resveratrol. These studies included cytotoxicity, DNA condensation, and DNA fragmentation assays.

3.4.1 Cytotoxicity

To determine the cytotoxic effect of nanoresveratrol on B16 cells, propidium iodide staining was performed. Resveratrol, nanoresveratrol and 5-FU were directly compared for their cytotoxic effects. Void nanoparticles were found to be biocompatible with B16 cells as indicated by reduced cytotoxicity. Nanoresveratrol proved to be more cytotoxic than resveratrol and 5-FU (Fig 4).

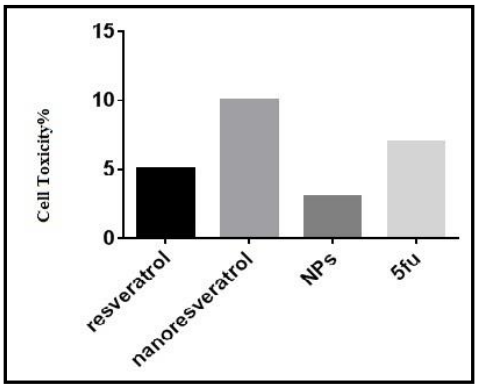

Figure 4. B16 cells treated or untreated with resveratrol, nanoresveratrol or 5-FU were stained with PI. *Uptake of PI indicates cytotoxicity. Nanoresveratrol showed maximum cytotoxicity.*

3.4.2 Apoptosis

Next, we determined the ability of nanoresveratrol to induce DNA condensation and DNA fragmentation in B16 cell line.

3.4.2.1 DNA Condensation: To assess DNA condensation, cells gown on cover slips, were treated with nanoparticles and stained with nuclear stain Hoechst, as described in Methods section. It was observed that the resveratrol loaded nanoparticles induced DNA condensation in B16 cells, indicative of apoptosis. In comparison, B16 cells treated with control void nanoparticles showed uniform staining (Fig 5). Furthermore, based upon the nuclear staining, apoptosis induced by nanoresveratrol was higher than in cells treated with free resveratrol. Apoptosis in both cases was time-dependent with a higher level seen at 12h versus 6h.

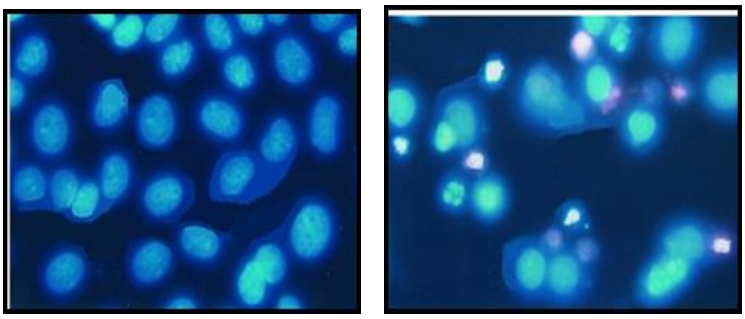

Fig 5 (a) **Fig 5 (b)**

Figure 5. Hoechst staining: *a) B16 cells treated with void nano particles showed uniform blue staining with Hoechst. b) B16 cells treated with nanoresveratrol showed bright blue staining with Hoechst.*

3.4.2.2 DNA Fragmentation: Fragmentation of DNA is a hallmark of apoptosis during which the fragmented DNA appears as a ladder. To assess DNA fragmentation, we carried out a DNA fragmentation assay to see the apoptotic effect of nanoresveratrol on B16 cells (Fig.6). Assay was performed after treatment of cells with different agents and controls. Post-treatment, DNA was extracted from B16 cells and electrophoresed to see the characteristic "DNA laddering" typical of apoptotic cells.

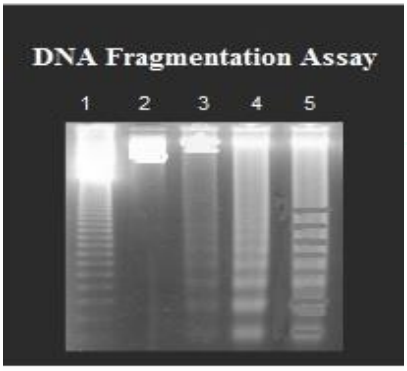

Figure 6. DNA Fragmentation Assay; *Lane-1 (DNA Marker), Lane-2 (B16 cell lines), Lane-3 (Resveratrol), Lane-4 (5-fluorouracil), Lane-5 (Nanoresveratrol)*

Cells incubated with the nanoresveratrol and 5-FU showed DNA laddering when compared to DNA from control cells (Fig.6;Lane 2). In addition, resveratrol treatment did not induce a strong ladder formation (lane 3), indicating modest apoptosis. In direct comparison with resveratrol, nanoresveratrol induced a clear DNA ladders indicating robust apoptosis. In addition, 5-FU also induced DNA fragmentation. Overall, this experiment clearly shows that calcium phosphate-encapsulated nanoresveratrol induces a robust apoptosis in melanoma cells.

Collectively all the above-mentioned studies show that calcium phosphate-encapsulated nanoresveratrol induces a potent pro-apoptotic effect in B16 melanoma cells. These studies further establish that the nanoresveratrol is superior to resveratrol with respect to anti-cancer effects. Nanoresveratrol therefore represents a candidate formulation to confirm these data *in vivo* models of the disease.

3.5 Antioxidant Activity

Resveratrol is a well-established antioxidant. In addition to examining the anti-cancer activities of resveratrol and nanoresveratrol, we directly compared their antioxidant activities through measurement of SOD and Catalase, which are two major antioxidant enzymes (Fig.7). Void-nano particles showed minimal to effect on these activities, as expected. Both SOD and Catalase activities were increased upon treatment with nanoresveratrol. Nanoresveratrol showed increase in antioxidant activities as compared to free resveratrol.

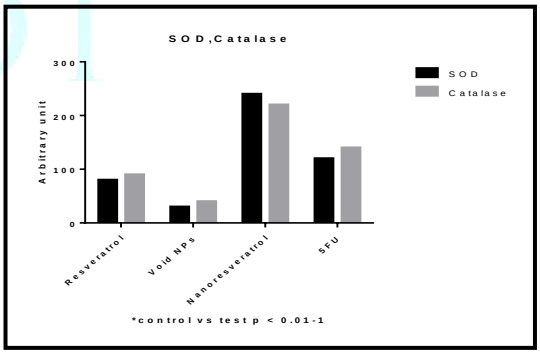

Figure 7. SOD and Catalase activity of Resveratrol, Nanoresveratrol and 5-FU. *Nanoresveratrol showed increased SOD and catalase activity*

Accumulating literature shows that resveratrol influences several biological processes. Resveratrol may help in the treatment of various diseases by various molecular and cellular mechanisms [5-14]. It is worth mentioning that antioxidant activity is associated with resveratrol but may not be required for its anti-cancer effects. However, antioxidant activity is a good indicator of the resveratrol activity. Our data clearly show that nanoresveratrol has superior anti-cancer and antioxidant activities as compared to free resveratrol.

4. CONCLUSION

In conclusion, we report here the synthesis and characterization of calcium phosphate encapsulated nanoresveratrol and determined the anti-cancer activity of nanoresveratrol in B16 murine melanoma cell line. We have observed that calcium phosphate nanoresveratrol shows a remarkably higher anti-cancer activity in B16 murine melanoma cell line as compared to resveratrol. The findings of the study indicate that nano formulation displays a superior efficacy as compared to free resveratrol warranting a further evaluation through in vivo models. To the best of our knowledge this is the first report showing the anticancer activity of calcium phosphate loaded nanoresveratrol in B16 murine melanoma cell line.

CONFLICT OF INTEREST

Authors do not have any conflict of interest.

ACKNOWLEDGEMENT:

The authors are thankful to Dr M.Samim, Jamia Hamdard University for providing facility & guidance on the preparation & characterization of nanoparticles.

REFERENCES

1. Pangeni R, Sahni JK, Ali J, Sharma S, Baboota S, Resveratrol: Review on therapeutic potential and recent advances in drug delivery, Expert opinion on drug delivery, 2014; 11:1-14.
2. Belguendouz L, Fremont L, Linard A, Resveratrol inhibits metal ion-dependent and independent peroxidation of porcine low-density lipoproteins, Biochemical Pharmacology,1997; 53(9): 1347-1355.
3. Brakenhielm E, Cao R ,Cao Y, Suppression of angiogenesis, tumor growth, and wound healing by resveratrol, a natural compound in red wine and grapes, FASEB Journal,2001; 15(10): 1798-1800.
4. Jang M, Cai L, Udeani GO, Slowing KV, Thomas CF, Beecher CW, Fong HH, Farnsworth NR, Kinghorn AD, Mehta RG, Moon RC, Pezzuto JM, Cancer chemopreventive activity of resveratrol, a natural product derived from grapes, Science,1997; 275(5297):218–220.
5. Rauf A, Imran M, Butt MS, Nadeem M, Peters DG, Mubarak MS, Resveratrol as an anti-cancer agent: A review, Critical Reviews in Food Science & Nutrition, 2018 ; 13;58(9):1428-1447.
6. Afaq F, Adhami VM, Ahmad N, Prevention of short-term ultraviolet B radiation-mediated damages by resveratrol in SKH-1 hairless mice , Toxicology and Applied Pharmacology, 2003; 186(1): 28-37.
7. Reagan S, Afaq F, Aziz MH, Ahmad N, Modulations of critical cell cycle regulatory events during chemoprevention of ultraviolet B-mediated responses by resveratrol in SKH-1 hairless mouse skin, Oncogene,2004; 23: 5151-5160.
8. Yang S, Wenshuai Li W, Sun H, Wu B, Ji F, Sun T, Chang H, Shen P, Wang Y, Zhou D , Resveratrol elicits anti-colorectal cancer effect by activating *miR-34c*-KITLG in vitro and in vivo, BMC Cancer, 2015; 15: 969
9. Shrotriya S, Agarwal R, Sclafani RA, A Perspective on Chemoprevention by Resveratrol in Head and Neck Squamous Cell Carcinoma. Advances in Experimental Medicine and Biology, 2015, 815: 333-348
10. Emmett MS, Dewing D , Pritchard-Jones RO: Angiogenesis and melanoma -from basic science to clinical trials, American Journal of Cancer Research, 2011; 1(7): 852-868.
11. Garvin S, Ollinger K, Dabrosin C, Resveratrol induces apoptosis and inhibits angiogenesis in human breast cancer xenografts in vivo, Cancer Letters, 2006; 231(1):113-122.
12. Cao Z, Fang J, Xia C, Shi X , Jiang BH, trans-3,4,5'-trihydroxystibene inhibits hypoxia-inducible factor 1alpha and vascular endothelial growth factor expression in human ovarian cancer cells, Clinical Cancer Research, 2004; 10 (15): 5253-5263.
13. Kimura Y, Okuda H: Resveratrol isolated from *Polygonum cuspidatum* root prevents tumor growth and metastasis to lung and tumor-induced neovascularization in Lewis lung carcinoma-bearing mice, The Journal of Nutrition, 2001; 131(6):1844-1849.
14. Kim SM, Kim SZ, Biological Activities of Resveratrol against Cancer. Journal of Physical Chemistry & Biophysics, 2018, 8:267.
15. Ndiaye M, Philippea C, Mukhtara, HB, Ahmada N, The Grape Antioxidant Resveratrol for Skin Disorders: Promise, Prospects, and Challenges, Archives of Biochemistry and Biophysics, 2011; 15; 508(2): 164–170.
16. Elshaer M, Chen Y, Wang XJ, Tang X, Resveratrol: An overview of its anti-cancer mechanisms, Life Sciences ,2018;207:340-349.
17. Lee SH, Koo BS, Park SY & Ki YM Anti-angiogenic effects of resveratrol in combination with 5-fluorouracil on B16 murine melanoma cells, Molecular Medicine Reports, 2015; 12: 2777-2783.
18. Zhao H, Han L, Jian Y, Ma Y, Yan W, Chen X, Xu H,Li L, Resveratrol induces apoptosis in human melanoma cell through negatively regulating Erk/PKM2/Bcl-2 axis, Onco Targets and Therapy, 2018; 11: 8995-9006.
19. Salehi B, Mishra AP, Nigam M, Sener B, Kilic M ,Sharifi-Rad , Fokou PVT ,Martin N , Javad Sharifi-Rad J, Resveratrol: A Double-Edged Sword in Health Benefits, Biomedicines, 2018; 6 (3): 91.
20. Singh CK, Ndiaye MA, Ahmad N, Resveratrol and cancer: Challenges for clinical translation, Biochim Biophys Acta, 2015; 1852(6): 1178–1185.
21. N. Oku, Oku N , Yamazaki Y, Matsuura M, Sugiyama M, Hasegawa M , Nango M, A novel non-viral gene transfer system, polycation liposomes, Advanced Drug Delivery Reviews, 2001, 52, 209-218.
22. Bondi ML, Azzolina A, Craparo EF, Lampiasi N, Capuano G ,Giammona G , Cervello M, Novel cationic solid-lipid nanoparticles as non-viral vectors for gene delivery, Journal of Drug Targeting, 2007; 15(4): 295-301
23. Midoux P, Pichon C, Yaouanc JJ, Jaffrès PA, Chemical vectors for gene delivery: a current review on polymers, peptides and lipids containing histidine or imidazole as nucleic acids carriers, British Journal of Pharmacology, 2009; 157(2):166-78.
24. Ortiz R, Prados J, Melguizo C, Arias JL, Adolfina RM, Álvarez PA, Caba O, Luque R, Ana Segura A, Aránega A, 5-Fluorouracil-loaded poly (ε-caprolactone) nanoparticles combined with phage E gene therapy as a new strategy against colon cancer, International Journal of Nanomedicine, 2012; 7: 195-107.
25. Li J , Mooney DJ, Designing hydrogels for controlled drug delivery, Nat Rev Mater, 2016; 1(12): 16071.
26. Bisht S, Bhakta G, Mitra SA, Maitra AN, pDNA loaded calcium phosphate nanoparticles: highly efficient non-viral vector for gene delivery, International Journal of Pharmaceutics, 2005; 288(1): 157-168.
27. Maitra A, Calcium phosphate nanoparticles: second-generation non-viral vectors in gene therapy, Expert Review of Molecular Diagnostics, 2005; 5(6):893-905.
28. Yang T, Wang L, Zhu M, Zhang L, Yan L, Properties and molecular mechanisms of resveratrol, a review, Pharmazie, 2015; 70: 501–506.
29. Moyano-Mendez JR, Fabbrocini G, de Stefano, D,Mazzella C, Mayol, L, Scognamiglio I, Carnuccio R, Ayal F, La Rotonda, MI, DeRosa G, Enhanced antioxidant effect of trans-resveratrol: Potential of binary systems with polyethylene glycol and cyclodextrin. Drug Development and Industrial Pharmacy, 2014; 40 (10):1300–1307.
30. Gokce EH, Korkmaz E, Dellera E, Sandri G, Bonferoni MC, Ozer O, Resveratrol-loaded solid lipid nanoparticles versus nanostructured lipid carriers: Evaluation of antioxidant potential for dermal applications, International Journal of Nanomedicine, 2012; 7:1841–1850.
31. Chen J, Wei N, Lopez-Garcia M, Ambrose D, Lee J, Annelin C, Peterson T, Development and Evaluation of Resveratrol, vitamin E, and epigallocatechin gallate loaded lipid nanoparticles for skin care applications, European Journal of Pharmaceutics and Biopharmaceutics, 2017; 117: 286–291.
32. Shen J, Zhou Q, Li P, Wang Z, Liu S, He C, Zhang C, Xiao P, Update on Phytochemistry and Pharmacology of Naturally occurring resveratrol oligomers, Molecules 2017; 22(12): 2050.

33. Duarte A, Martinho A, Luís Â, Figueiras A, Oleastro M, Domingues FC, Silva F, Resveratrol encapsulation with methyl-β-yclodextrin for antibacterial and antioxidant delivery applications, LWT Food Science and Technology, 2015; 63:1254–1260
34. Calcium phosphate nanoparticle mediated genetic transformation in plants, Naqvi S, Maitra AN,. Abdin MZ, Akmal M , Samim M, Journal of Materials Chemistry, 2012; 8: 3500
35. Cao B, Xu H ,Mao C, Transmission Electron Microscopy as a Tool to Image Bio-Inorganic Nanohybrids: The Case of Phage-Gold Nanocomposites, Microscopy Research Techniques, 2011; 74(7): 627–635.
36. Carlo SD, Harris JR, Negative staining and Cryo-negative Staining of Macromolecules and Viruses for TEM, Micron, 2011; 42(2):117–131.
37. Latt SA, Stetten G, Juergens LA, Willard HF, Scher CD , Recent developments in the detection of deoxyribonucleic acid synthesis by 33258 Hoechst fluorescence, Journal of Histochemistry and Cytochemistry, 1975; 23 (7): 493–505.
38. Latt SA, Stetten G , Spectral studies on 33258 Hoechst and related bisbenzimidazole dyes useful for fluorescent detection of deoxyribonucleic acid synthesis, Journal of Histochemistry and Cytochemistry,1976; 24 (1): 24–33.
39. Weydert CJ, Cullen JJ, Measurement of superoxide dismutase, catalase, and glutathione peroxidase in cultured cells and tissue, Nature Protocols, 2010; 5(1): 51–66.